

Estimation of the Air Flow Behavior in the 3D Solid and Numerical Models of Nose

Gennadij Lukyanov, Anna Rassadina

ITMO University,
Saint-Petersburg Electrotechnical University 'Leti'
Saint-Petersburg, Russian Federation
gen-lukjanow@yandex.ru, a.a.rassadina@gmail.com

Roman Neronov

JSC "Modern Medical Technologies"
Saint-Petersburg, Russian Federation
nrvspb@mail.ru

Abstract— Respiratory physiology depending on the shape of the nasal cavity was studied. Experiments on solid and numerical models show the difference at tidal exchange depending on the shape of the nasal cavity.

I. INTRODUCTION

The nasal cavity is a complex miniature geometric shape of irregular cross-section. Bony turbinates divides the cavity into four nasal passages. All that makes breathing study difficult.

There are three main directions in the study of respiration. These are experimental studies on full-scale models of the nose, these are numerical simulations, and these are studies on living material — humans, animals. By mixed research can include attempts to perform research on the nasal cavities of corpses.

The first full-scale models was produced in 20-s and 30-s of the previous century (authors Mink P.(1920), Hofbauer (1921), Takahashi K. (1923), Businger O. (1936), Scheideler J. (1938)) [1-3]. As a rule – these are only visual observations of stained liquid or smoke moving in the solid model. And the model could be sized for the convenient observation. So the authors [2-3] used rectangular-shaped boxes, inside which it was possible to create motion interference defining the flow angle and its movement.

The development of computer technology, the emergence of new software products has shifted the focus of research in the field of numerical modeling. The first 3D-model of a nasal half truncated in the nasopharynx area was created in 1995 (Keyhani and others) [4]. In the last decade we see an outbreak of works on this theme. Some of them are represented in the list [5–7]. Depending on the variability or constancy of the modelled flow parameters to time, we have to select two large groups which represent the stationary (independent on time) or unsteady flow (considering changes of flow in time) simulation. The stationary models use e. g. mass air flow rate [5] or pressure drop [6] as a boundary condition. Unsteady models also use boundary conditions as stationary ones with the conditions of the fixed-rate flow in the enter into the nasal cavity [7].

When performing research in humans, the main difficulty is related to the impossibility of placing diagnostic sensors directly in the departments of the nasal cavity. In the generally accepted medical diagnostic equipment, the measurement of

the physiological parameter of respiration (nasal resistance) is determined by the ratio of pressure drop to flow in the tube supplied to the nasal cavity, as it is done in the anterior active rhinomanometer. Either these are indirect measurements as in the method of acoustic rhinometry. However, the problem can be solved by applying miniature high-speed sensors, the sensitive elements of which can be placed in the region of the nasal vestibule. So we developed a number of prototypes, the construction and operation of which are given in [8-10].

The movement of air flow within the nasal cavity is very actual task. Research in this area will expand our knowledge of the physiology of respiration. These studies have a high practical significance for the improvement of existing diagnostic methods. They are relevant for surgical intervention. It is very important to understand the movement of air flow within the nasal cavity for surgical intervention. The modern medicine tends is minimizing harm, achieving the best positive effect of the knife. Therefore it is necessary to understand: how air should move in the nasal cavity during the breathing.

The result of the proposed research is planned to be used as the basis for the implementation of the "virtual operation" program. It is assumed that prior to surgical intervention, mathematical modeling of the upcoming surgery will be performed on a 3D model of the patient's nasal cavity, created according to computer tomography (this is the "virtual operation"). Such an operation will allow minimizing the surgical effect, which can be achieved on the basis of understanding the features of the the particular nasal cavity anatomy influence on the movement of air in the cavity during breathing (understanding of norms and pathology).

The ways of air movement in the nasal cavity during breathing are extremely individual. There are three evolutionarily formed shapes of the nasal cavity. They are: platyrhine, mesorhine, leptorhine.

Scientific community shows that the differences at the air flow movement depending on the shape of the external nose [11-15]. However, the shape of the external nose does not always correspond to the shape of the nasal cavity. For this reason we undertake a study of air movement during the breathing at the leptorhine-, meso-, and platyrhine- cavity of nose. The shape of the nasal cavity was determined by the method [16].

Nose shape effect to the air moving is yet one crucial task of study.

The goal of the work is the estimation of the air flow moving through the 3D solid models of lepto-, meso-, and platycavity of nose at the breathing simulation and comparison the results of the study with the numerical simulation of air flow moving.

This information can be used to refine existing models of the processes and, in turn, allows better understand the evolution of the processes, allows to receive more accurate assessment of the human condition.

Numerical and 3D-solid nasal cavities models were reconstructed according to computer tomography data (CT).

3D-solid models were created by 3d-printer technology at the scale 1:1 upon the same computer tomography data.

Numerical models were used to simulation in an ANSYS package. Air was considered as incompressible quasi-viscous liquid at modeling. The motion of air flow was described through a partial differential system (the Navier-Stokes equations) [17].

This work is initiative. Its goal is to determine further research directions for fundraising.

II. MATERIALS AND METHOD

A. The generation of models prototypes

The prototypes of models were created by the geometrical model of human internal nasal channels of lepto-, meso-, and platy- cavity types of nose. These models became the basis for numerical modeling and for 3D printer printing of solid models. They were reconstructed by the patients CT scans with the help of specialized Mercury Amira software package at the “Modern medical technology” medical holding (St. Petersburg). The three-dimensional geometric model image for mesocavity type of nose is shown in Fig. 1.

For performed numerical simulation, geometric models had been segmented to the “entrance”, “exit” and “wall” boundaries (Fig. 1b). These boundaries were carried out with the help of Altair Hypermesh software package.

Then, every geometric model was imported together with segmentation parameters in Ansys software to STL file (Fig. 1b). In Ansys Icem CFD software, an irregular surface and volume finite element mesh was sequentially constructed with the following parameters

- The maximum size of the final element edge - 0.4 mm. It was based on two reasons – (1) minimum grade value of tomograph; (2) - the capabilities of the computing resource;
- $4.5 \cdot 10^6$ triangular surface elements and $3.9 \cdot 10^7$ bulk tetrahedral elements.

Numerical modeling was performed using Ansys Fluent software.

For performed experiments, two types of 3D solid models has been created.

- Opaque models that fully reproduce the internal structure of the nasal cavity.
- Transparent models of the right half of the nasal cavity without the maxillary sinus.

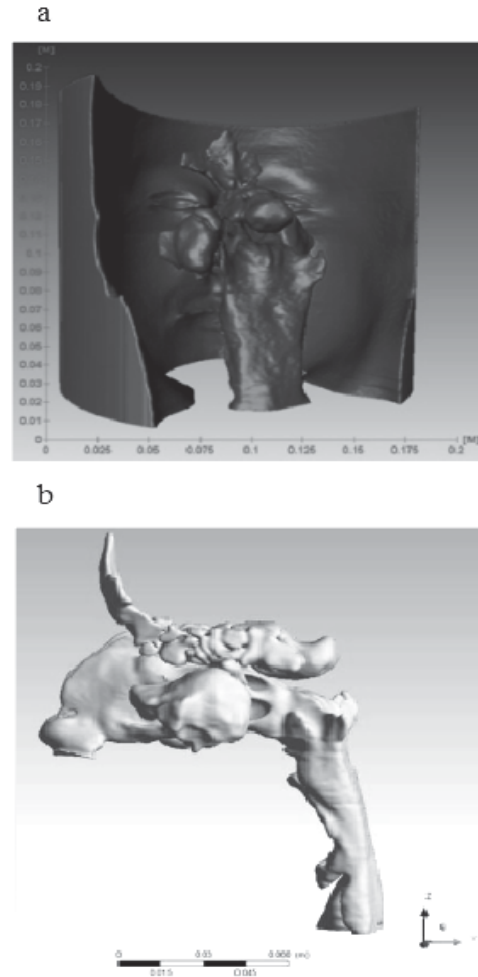


Fig. 1. Geometric models: (a) base model; (b) edit model

Opaque models had been used at experiments for measurement air flow parameters. In this case, pressure fluctuations were taken as a parameter of the air flow.

Transparent models had been used at experiments for visualization of air flow in nose cavity.

B. Numerical model

It is known that the movement of the air flow during the respiratory cycle in the nose cavity is unsteady. There is a conversion from laminar flow to turbulent vortices and back. All this is determining by the structure of the nasal cavity, where there are areas with flow separation and recirculation zones. In this case, a non-stationary calculation should be performed, which allows to obtain turbulent pulsations.

There are three main groups of the mathematical models, the use of which is possible with the implementation of the numeral experiment [18]

- RANS model (Reinolds-averaged Navier Stokes) - mathematical models, based on the solution of the Navier-Stokes time-averaged equations.
- LES model (Large Eddy Simulation) and its derivatives (DES, DDES, IDDES et al.), suggesting a direct numerical calculation of predetermined value turbulent flow parameters.
- DNS model (Direct Numerical Simulation), based on the direct numerical solution of the motion equations for all spatiotemporal characteristics with resolve of all turbulent structures scales within the flow.

Required analysis might be executed by the direct numerical simulation more completely. Today, however, the solution of this problem is severely restricted by the modern computer power possibilities: in spite of the Reynolds numbers (Re) have the boundary values between laminar and turbulent regimes in the nasal cavities, the necessity of mesh generation for the DNS method with the number of cells proportional Re^3 makes the values Re at 2×10^3 unacceptable high, and the total number of the mesh elements in this connection come up to the order - 10^{10} . As part of today's opportunities the best solution of the problem is in the framework of the DES, DDES, IDDES and the others derivatives of the LES model. In this case, the number of the calculated elements in the mesh will be of the order of 3.5^7 value, which is accessible for the calculation.

Among the methods for calculating turbulent flows, a model of Detached Eddy Simulation Spalart-Allmaras (DES-SA) is chosen. An non-stationary calculation of the thermal and hydrodynamic parameters of the air flow — velocity, temperature and pressure - was made for the respiratory cycle.

In order to describe a fluid flow the Navier-Stokes equations was used. The equation system includes continuity equation and equations for the flow velocity.

The continuity equation is

$$\frac{\partial \rho}{\partial \tau} + \frac{\partial \rho u_j}{\partial x_j} = 0 \quad (1)$$

The motion equation is

$$\frac{\partial \rho u_j}{\partial \tau} + \frac{\partial \rho u_j u_i}{\partial x_j} = \frac{\partial P}{\partial x_i} + \frac{\partial \tau_{ij}}{\partial x_j} \quad (2)$$

where, u_i , u_j - are the flow velocity component, ρ is the density, τ_{ij} - is the deviatoric stress tensor.

The most significant advantage of DES algorithm over RANS method is based on possibility to gather the information on high frequency eddies inside the flow which is gained by replacing of time filtration (RANS models) with the spatial filtration (DES methods).

The mathematical formulation of velocity field vector filtration $\bar{\mathbf{u}}(\mathbf{x}, t)$ is

$$\bar{\mathbf{u}}(\mathbf{x}, t) = \int \mathbf{G}(\mathbf{r}, \mathbf{x}) \mathbf{u}(\mathbf{x} - \mathbf{r}, t) d\mathbf{r} \quad (3)$$

here $\mathbf{G}(\mathbf{r}, \mathbf{x})$ - filtration function.

The width of the filter determining the function $\mathbf{G}(\mathbf{r}, \mathbf{x})$ can be determined explicitly, or with the size of the finite element mesh. Equations (1) and (2) filtered according to the equation (3) can be simplified to this form

$$\begin{aligned} \frac{\partial \rho \bar{u}_i}{\partial \tau} + \frac{\partial \rho \bar{u}_i \bar{u}_j}{\partial x_j} = & - \frac{\partial}{\partial x_i} \left(\bar{p} + \frac{2}{3} \mu \frac{\partial \bar{u}_k}{\partial x_k} \right) + \\ & + \frac{\partial}{\partial x_i} \left(\mu \left(\frac{\partial \bar{u}_i}{\partial x_j} + \frac{\partial \bar{u}_j}{\partial x_i} \right) \right) - \rho \tau_{ij}^r \end{aligned} \quad (4)$$

where τ_{ij}^r is the stress deviator tensor. This parameter has to be determined in order to solve the equations (4).

Simulation of the stress deviator tensor is performed by so-called eddy-viscosity subgrid-scale models, such as the Smagorinsky model. This model contains the hypothesis of proportionality of the stress deviator tensor to strain velocity tensor of filtered area and is structurally similar to the Boussinesq hypothesis.

In accordance to DES method the linear scale l_{RANS} is replaced with the following ratio:

$$l_{DES} = \min \{ l_{RANS}, C_{DES} \Delta \} \quad (5)$$

where, l_{DES} - DES linear scale, C_{DES} - constant, Δ - a filter size, is determined as:

$$\Delta = \max \{ \Delta_x, \Delta_y, \Delta_z \} \quad (6)$$

where, $\Delta_x, \Delta_y, \Delta_z$ is the finite element size.

The replacement result is congruence $l_{DES} = l_{RANS}$ and the DES model performs functions as a RANS model if the size of filter (computational mesh) is too crude and $C_{DES} \Delta > l_{RANS}$.

Otherwise, the DES model is transformed into LES model and complies with solution of filtered equations (4). Thus, DES method allows reaching significantly transient solution of the question problem.

The following boundary conditions were assumed

The pressure in the vestibule of nose ("entrance")

$$P = 0 \quad (7)$$

The air flow velocity spatial components on a "wall"

$$u_1 = u_2 = u_3 \quad (8)$$

The pressure in the nasopharynx ("exit") at an inspiration

$$P = 50 \cdot \cos \left(\pi \left(0.87\tau + 0.5 \right) \right) + 50 \quad (9)$$

The pressure in the nasopharynx (“exit”) at an expiration

$$P = 50 \cdot \sin\left(\pi\left(1.18\tau + 0.5\right)\right) - 50 \quad (10)$$

C. Experiment modelling

1) *Opaque models:* The material of one of the printed models is gypsum. The air motion imitation of breathing was performed through a tube that was fixed to the nasopharynx area of the model. The piezoresistive pressure sensors through thin shunt tubes were connected with multiple places of the solid model for the pressure drop fixing of air flow in time. The locations of the shunt tubes to the pressure sensors are shown in the Fig. 2.

Signals received from pressure sensors supplied to the data automation subsystem, which control and synchronize the sensors. Settings and data recording performed by software provided by the manufacturer.

Data processing was performed at Matlab mathematical modeling package. For data processing was written the software application which allow to convert voltage output value of the sensors in Pascal (Pa), filter data, delete steady component at the pressure transducer readings, which the sensors produces as a default, display depending on the time domain.

2) *Transparent models:* These models were created by 3d-printer technology at the scale 1:1 upon the same computer tomography data from polished plastic. Models presented at the Fig. 3.

At the experiment the breathing was modeled in a certain way: an air flow with a temperature of 35 ° C and a peak flow rate of 10 l/min was provided using a PVC tube that was putting at the nasopharynx. The air flow distribution was estimated using the Testo 890 thermal imager at the temperature range of 20-30 ° C. The experimental setup is shown in the Fig. 4.

This method was used for the study of airflow moving for the first time; so before application of the method, we performed its testing.

The infrared imaging method was tested by using a sensor system. This system included four response speed copper-constantan thermocouples and data acquisition device (Fig. 5).

Thermocouples 1, 3, 4 were installed through fine diameter bore (0.5 mm) at the inner wall of one of the models. Thermocouple 2 was located at the outer wall of the model.

The data obtained from the thermal imager and four thermocouples were processed by the MatLab software package. The results showed

- 1) The data of the thermal imager correspond to the thermocouple fluctuations at the given points (Fig. 4c).
- 2) The inspiration - expiration period was 16 seconds.
- 3) The delay time between the results of the thermal

imager and the thermocouples 1, 3, 4 was 2.4 s. These thermocouples were located inside the model.

4) The delay time between the results of the thermal imager and the thermocouple 2 was 0.1 s. The thermocouple was located on the outer surface of the wall.

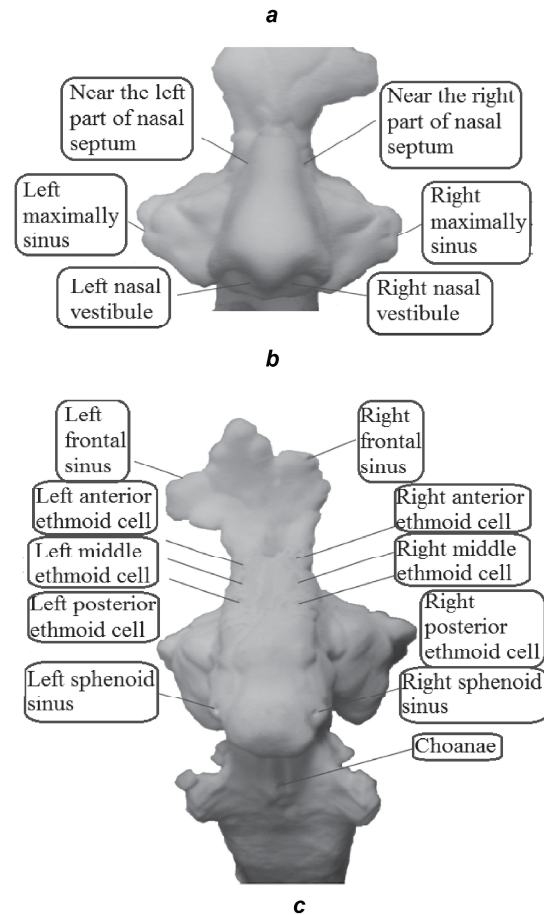
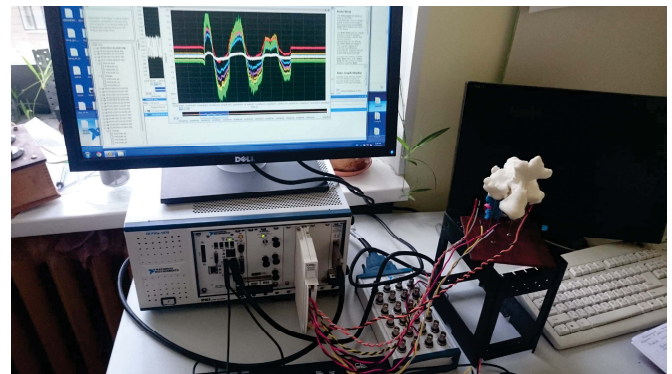
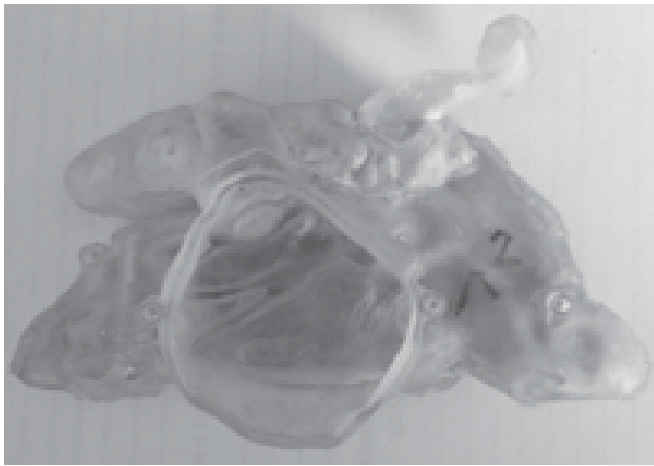
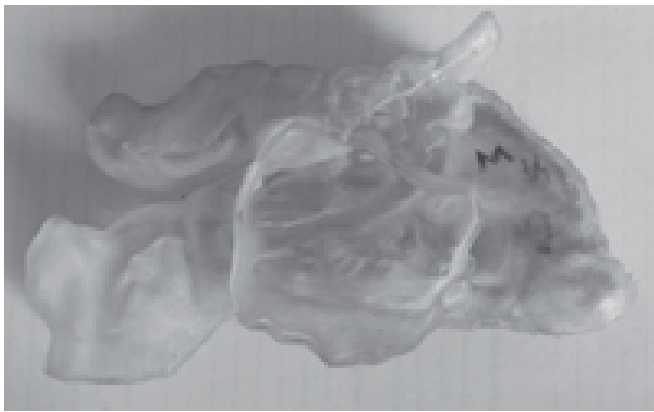


Fig. 2. The places of location thin shunt tubes for measuring of pressure at the artificial solid model of human nose cavity: (a) general view of the measurement setup with measurement result (b) front view of artificial model; (c) back view

Comparing the inspiration - expiration period and the delay time, it can be concluded that the wall of the model quick heats and cools.



a



b

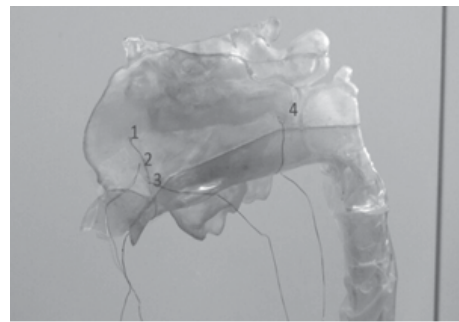


c

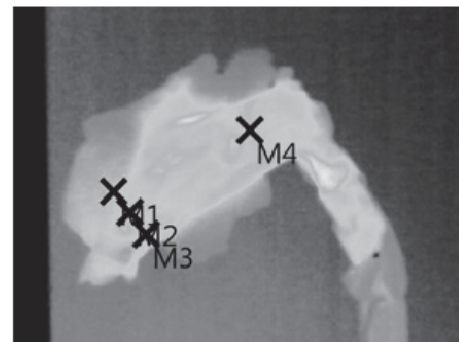
Fig. 3. 3D-solid models of right cavity of nose: a – lephthorcavity, b – mesorcavity, c – platycavity



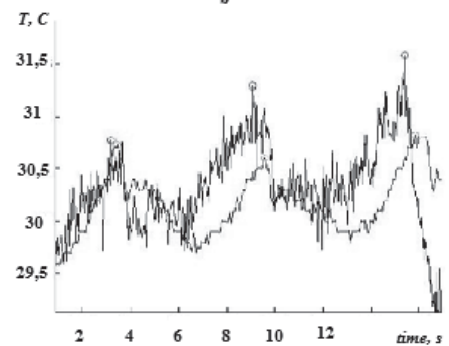
Fig. 4. The experimental setup for thermographic research



a



b



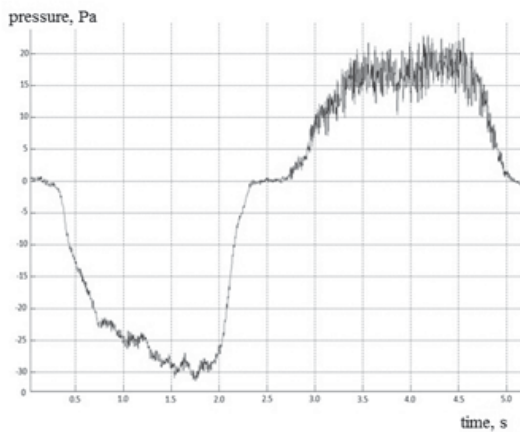
c

Fig. 5. (a) Location of thermocouples at the Sensor system; (b) points for measurements with a thermal imager; (c) comparison of measurement results by thermocouple (black) and thermal imager (blue)

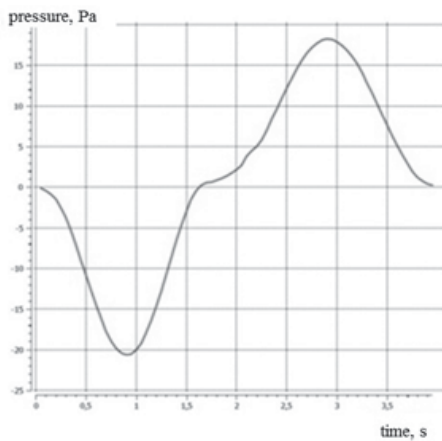
IV. RESULTS

A. Comparison of measurement results of numerical model and opaque models

The Fig. 6a shows the result of experimental measurement of pressure drop in solid model of human cavity. The pressure drop was measured in a vestibule of the nose (nostrils). The Fig. 6b shows the result of numerical simulation for the corresponding computer model of the nasal channels (vestibule of the nose). The results of numerical simulations are correlated with the experimental results. Note that the numerical calculation of nonstationary boundary conditions was given for "exit" (the region of the nasopharynx). The similarity of the waveforms and amplitudes of computer and solid models suffer to do the conclusion about the adequacy of the used computer model of the nasal channels and method of computation of hydrodynamic problem.



a



b

Fig. 6. Results of the measurement and the modeling of pressure drop in the vestibule of the nose: (a) – solid model; (b) – numeral computation

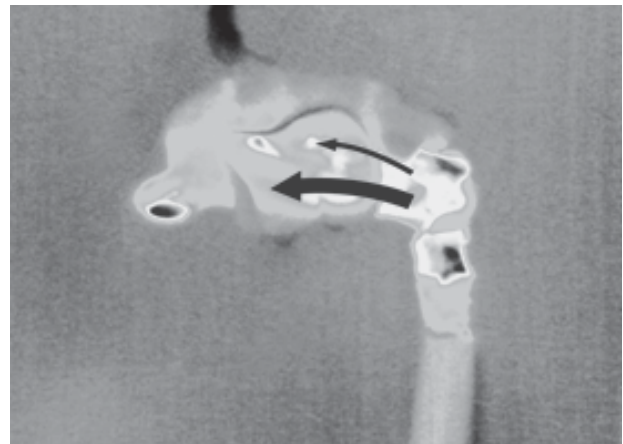
B. Comparison of measurement results of numerical model and transparent models

The results of numerical simulation and thermography are shown in Fig. 7, 8, 9.

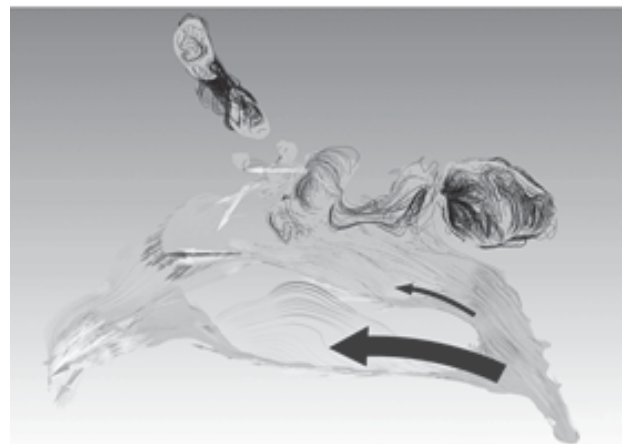
At the Fig. 7 one can see in lepthorcavity form with inspiration and expiration, the movement of air prevails through the lower regions of the model.

Fig. 8 show results of measurements at mesorcavity form. During inspiration, the main part of the air flow was concentrated in the lower lobes of the model, while expiration the air was evenly distributed between the middle and lower regions.

In the platyrcavity form during inspiration, there was an movement of air to the upper sections; when at the expiration, the air is evenly distributed throughout the area of the nasal passage (Fig. 9).



a



b

Fig. 7. Results (a) thermography and (b) numerical modeling at lepthorcavity form of nose

V. CONCLUSION

The study of the liquid or gas flow movement in the irregularly shaped channels is a non-trivial task. Such channels, considered by us on the example of the nasal cavity, are characterized by the presence of a large number of areas with flow separation, the presence of recirculation zones.

Studies are hampered by the miniature dimensions of such channels. Two types of simulation, numerical and experimental, were performed. A feature of numerical simulation was the implementation of non-stationary calculations using a DES model that, on the one hand, allows one to observe small eddies in the flow, and on the other hand, is characterized by the presence of an acceptable size of the computational grid for calculations (about 3.57 elements). Note that among the turbulent models that are also used to study, the RANS models does not allow to see small eddies in the flow, and the DNS models has a computational grid with a very large number of elements (about 10^{10}), which requires calculations on super-powerful computers. Since numerical simulation depend heavily on the model for calculations choice, and on model initialization, the results of numerical simulation must be verified by experimental studies. Experimental studies using opaque models pressure fluctuations at some points within the solid model of the nasal cavity was obtained. Pressure fluctuations at some points within the opaque solid model of the nasal cavity were obtained. On the basis of these data, the requirements for specifying the initial conditions when performing numerical simulations were formulated. Further, a series of experiments was carried out with a thermal imager and transparent models of the right half of the nasal cavity. The visual images of the temperature field near the septum of the nasal cavity model were obtained. These results were compared with numerical simulation data. Comparison of the results led to the following conclusions from the study

- 1) Separate a wide nose (platycavity form of nose), it should be noted that when inhalation and exhalation, the air tends to the upper areas of the nasal cavity.
- 2) In a narrow nasal cavity (leptocavity form of nose), the air, during inhalation and exhalation, moves along the bottom and middle parts of the nasal cavity.
- 3) In the middle nose (mesocavity form of nose) during inspiration, the main part of the air flow was concentrated in the lower lobes of the model, while expiration the air was evenly distributed between the middle and lower regions.

ACKNOWLEDGMENT

We would like to thank our programmer Aleksey Voronin to his work and collaboration in numerical simulation. Our work would not have taken place without the participation of this wonderful specialist.

REFERENCES

[1] B. M. Sagalovich, *Physiology and Pathophysiology of the Upper Respiratory Tract* Moscow: Meditsina. 1964.
 [2] G. Mlynski, S. Grutzenmacher, S. Plontke, B. Mlynski, and C. Lang, "Correlation of nasal morphology and respiratory function", *J. Rhinology*, 2001, 39, 197-201.
 [3] G. Mlynski, S. Grutzenmacher, S. Plontke, W. Grutzmacher, B. Mlynski, P. C. Lang "A method for studying nasal air flow by means of fluid dynamics experiments", *J. z. Med. Phy.*, 2000, 10, 207-214.
 [4] K. Keyhani, P. W. Scherer, and M. M. Mozell, "Numerical simulation of airflow in the human nasal cavity", *J. Biomech. Eng.*, 1995, 117, 429.

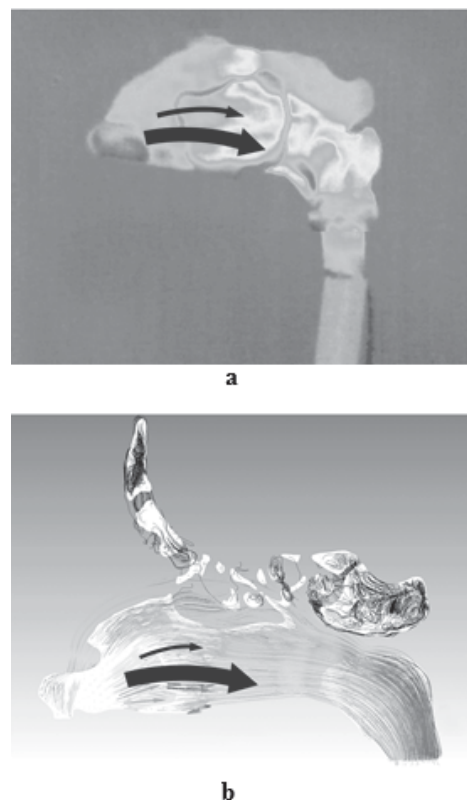


Fig. 8. Results (a) thermography and (b) numerical modeling at mesocavity form of nose

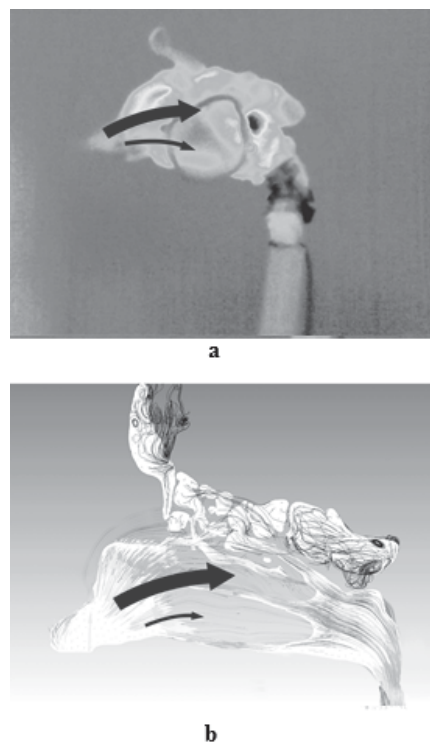


Fig. 9. Results (a) thermography and (b) numerical modeling at platycavity form of nose

- [5] J. Wen, K. Inthavong, Z. F. Tian, J. Y. Tu, C. L. Xue and C. G. Li, "Airflow Patterns in Both Sides of a Realistic Human Nasal Cavity for Laminar and Turbulent Conditions", in *Proceedings of the 16th Australasian Fluid Mechanics Conference*, Crown Plaza, Gold Coast, Australia, 2007, pp. 68-74.
- [6] K. Zhao, P. Dalton, G. C. Yang, and P. W. Scherer, "Numerical modeling of turbulent and laminar airflow and odorant transport during sniffing in the human and rat nose", *J. Chem. Senses*, 2006, 31 (2), 107-118.
- [7] J. Pennecot, M. Ruetten, R. Kessler, and C. Wagner, "CFD Mesh of the Human Nose and Flow Simulation", in *Proceedings of the 8th World Congress on Computational Mechanics*, Venice, 2008.
- [8] G. Lukyanov, A. Rassadina, V. Usachev, "Comparison and the analysis of the processes of the movement of air through the human breathing system and its natural model", 2005, *2005 International Conference on Physics and Control, PhysCon 2005, Proceedings*
- [9] A.G. Malyshev, N.K. Zhumashev, G.N., Lukyanov, K.D. Mynbaev, A.A. Rassadina, "Application of a LED-photodiode optocouple for the study of human respiratory function", *Journal of Physics: Conference Series*, 2015
- [10] Lukyanov G.N., Rassadina A.A., Makarov S.L. "A new method and a sensor for diagnosis of the respiratory diseases", *2nd International Scientific Symposium "Sense. Enable. SPITSE"* (St.Petersburg, 22June-03July 2015) - 2015, pp. 219-222
- [11] J. Znu *A numerical study of airflow through human upper airways*. Singapore: National University of Singapore. 2012. 192 p.
- [12] J. H. Zhu, H. P. Lee, K. M. Lim, Sh. J. Lee, D. Y. Wang, "Evaluation and comparison of nasal airway flow patterns among three subjects from Caucasian, Chinese and Indian ethnic groups using computational fluid dynamics simulation", *J. Respiratory Physiology & Neurobiology*, 175 (2011), 62-69
- [13] J.A. Keeler, A. Patki, C.R. Woodard, D.O. Frank-Ito, "A Computational Study of Nasal Spray Deposition Pattern in Four Ethnic Groups", *J. Aerosol Med Pulm Drug Deliv*. 2016 Apr;29(2):153-66. doi: 10.1089/jamp.2014.1205.
- [14] K. Zhao, J. Jiang, "What is normal nasal airflow? A computational study of 22 healthy adults", *J. Int Forum Allergy Rhinol*. 2014 Jun;4(6):435-46. doi: 10.1002/alr.21319
- [15] X.B. Chen, H.P. Lee, V.F. Chong, Y. Wang de, "Impact of inferior turbinate hypertrophy on the aerodynamic pattern and physiological functions of the turbulent airflow - a CFD simulation model", *J. Rhinology*. 2010 Jun;48(2): 163-8. doi: 10.4193/Rhin09.093.
- [16] R. V. Neronov, G. N. Luk'yanov, A. A. Rassadina, A. A. Voronin, A. G. Malyshev, "The effect of the nasal cavity form on air flow distribution during inhalation", *J. Russian Otorhinolaryngology*, 2017, 1 (86), 83-94
- [17] G.N. Lukyanov, A.A. Voronin, A.A. Rassadina, "Simulation of convective flows in irregular channels on the example of the human nasal cavity and paranasal sinuses", *J. Technical Physics. The Russian Journal of Applied Physics*. 2017, 62 (3), 484-489.
- [18] A. Voronin, G. Luk'yanov, E. Frolov "Detached-eddy simulation of turbulent airflow", *Scientific and Technical Journal of Information Technologies, Mechanics and Optics*, 2014, №1 (89) 187-192